

A tutorial on Bargmann invariants

Ernesto Galvão

Quantum and Linear-Optical Computation group

International Iberian Nanotechnology Laboratory (INL)

and (on leave) Universidade Federal Fluminense (Brazil)

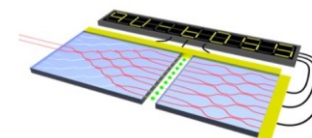


INSTITUTO DE FÍSICA
Universidade Federal Fluminense

- Funding



Funded by
the European Union

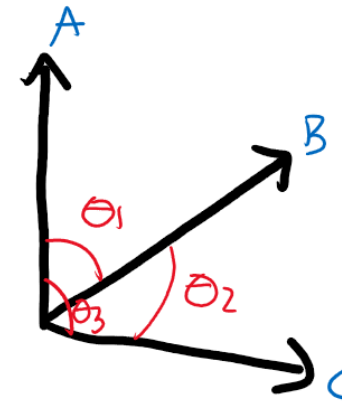


FCT
Fundação para a Ciência e a Tecnologia
MINISTÉRIO DA CIÊNCIA, TECNOLOGIA E ENSINO SUPERIOR

- Unitary invariants to characterize relational quantum information
- Measuring the invariants
- Nonclassicality of...
 - ...overlaps: coherence and contextuality inequalities
 - ...higher-order invariants: applications

Relational = unitary-invariant properties of a set of states

- Geometrical in character – they're about the relative orientation of the states



- Mathematical result: all unitary-invariant properties can be written in terms of **k-th order Bargmann invariants**: [Chien, Waldron. SIAM J. Discrete Math. 30 (2), 976 (2016)]

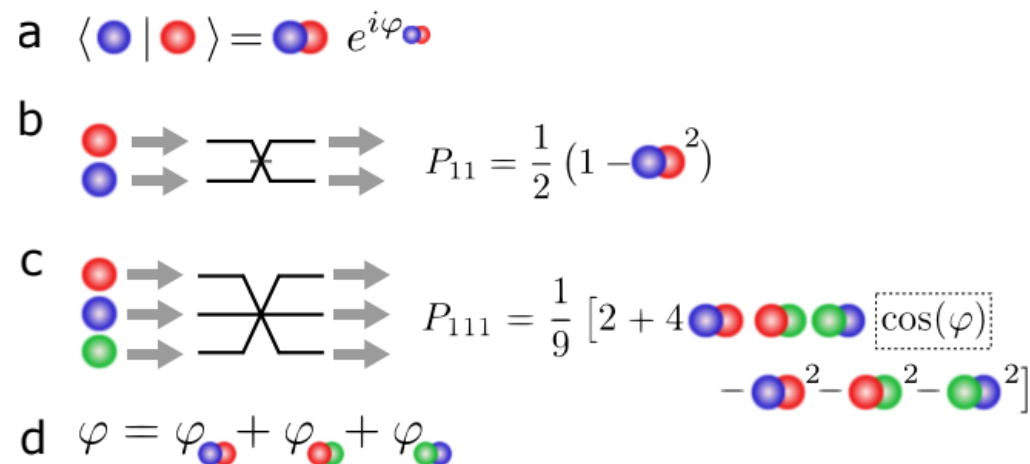
$$\Delta_{ABC\dots K} = \langle A|B\rangle\langle B|C\rangle\langle C|D\rangle\dots\langle K|A\rangle$$

$$\Delta_{ABC\dots K} = \text{Tr}(\rho_A\rho_B\rho_C\dots\rho_K)$$

- We call *relational quantum information* any property of a set of projectors that is unitary-invariant. Examples:
 - Probabilities in prepare-and-measure scenarios
 - Success rate in unambiguous state discrimination
 - Dimension of spanned Hilbert space

Bargmann invariants – where they show up

- Probabilities in quantum mechanics: $p_{\rho P} = \text{Tr}(\rho P)$
- Compatibility between two projectors: P_1, P_2 compatible iff $\text{Tr}(P_1 P_2) = 0$.
- They determine output probabilities of linear-optical experiments with partial photonic indistinguishability

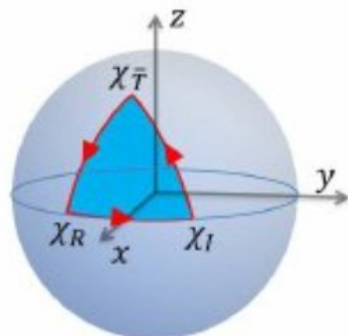


[from A. J. Menssen, et al., PRL 118, 153603 (2017)]

- Example: d=3 QFT with three input photons, each with their own internal spectral functions. Output is a function of overlaps and phase φ of 3rd-order invariant of the 3 spectral functions

- Geometric phases are phases of Bargmann invariants

[Simon, Mukunda, Phys. Rev. Lett. 70, 880 (1993)]



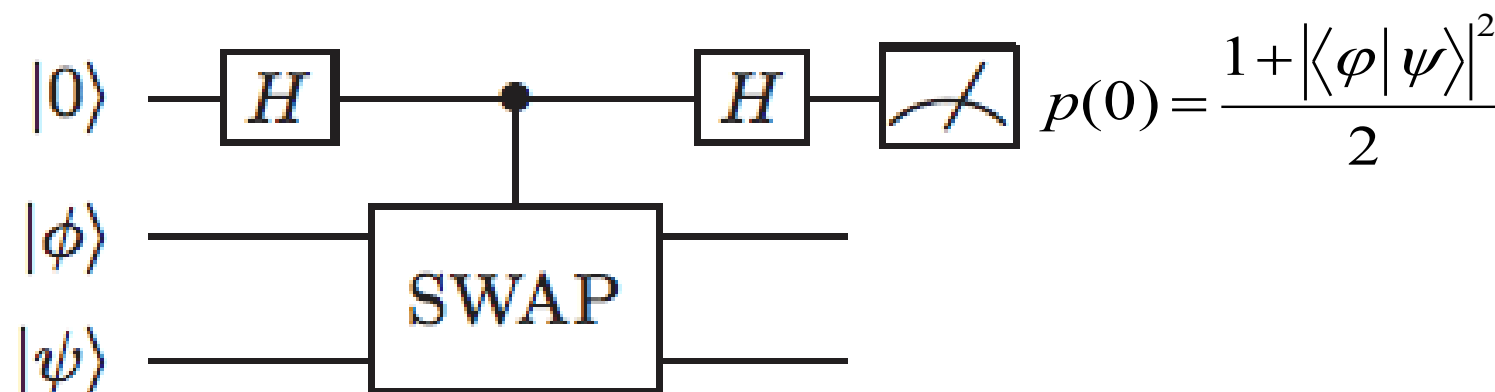
- Phase of Δ = Pancharatnam (geometric) phase acquired by cyclic sequence of projective measurements

Circuits to measure Bargmann invariants

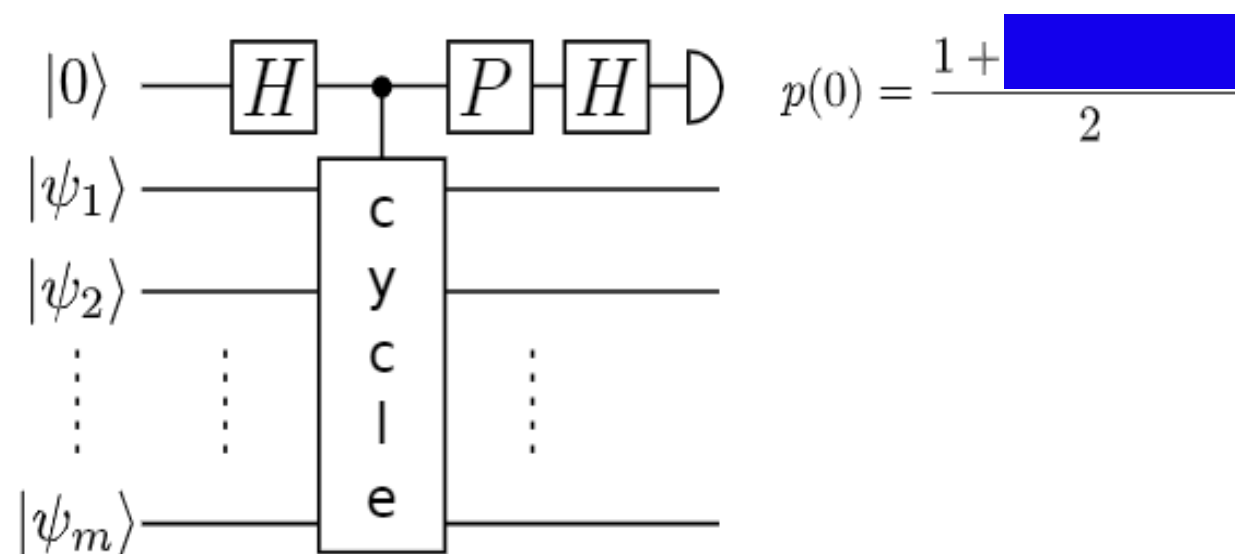
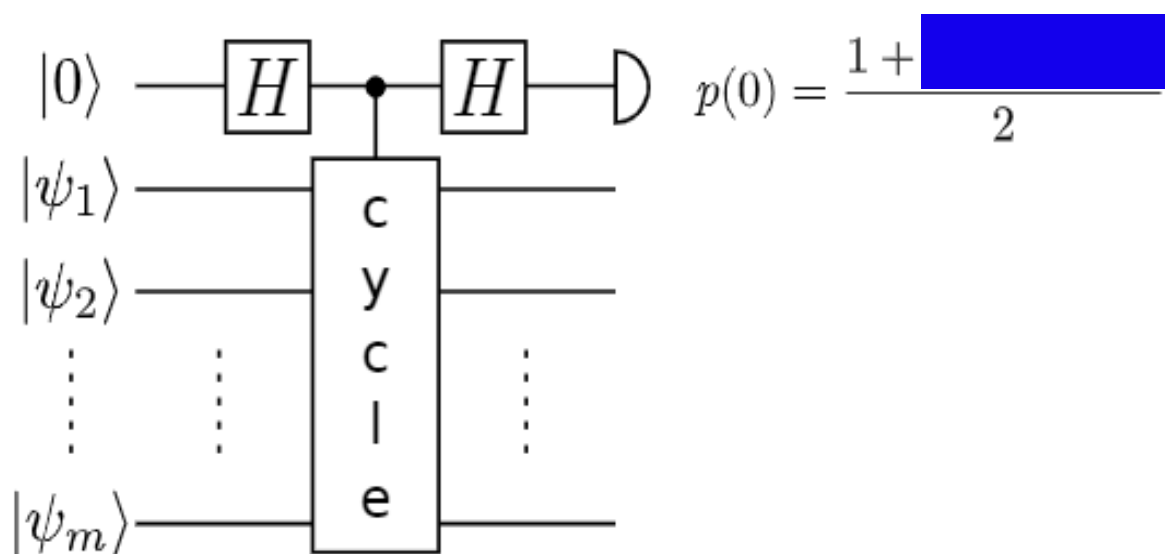
[Oszmaniec, Brod, EG, arXiv:2109.10006]

- Known result: SWAP test circuit measures simplest invariant, the two-state overlap:

$$\Delta_{AB} = |\langle A|B \rangle|^2 = \text{Tr}(\rho_A \rho_B)$$



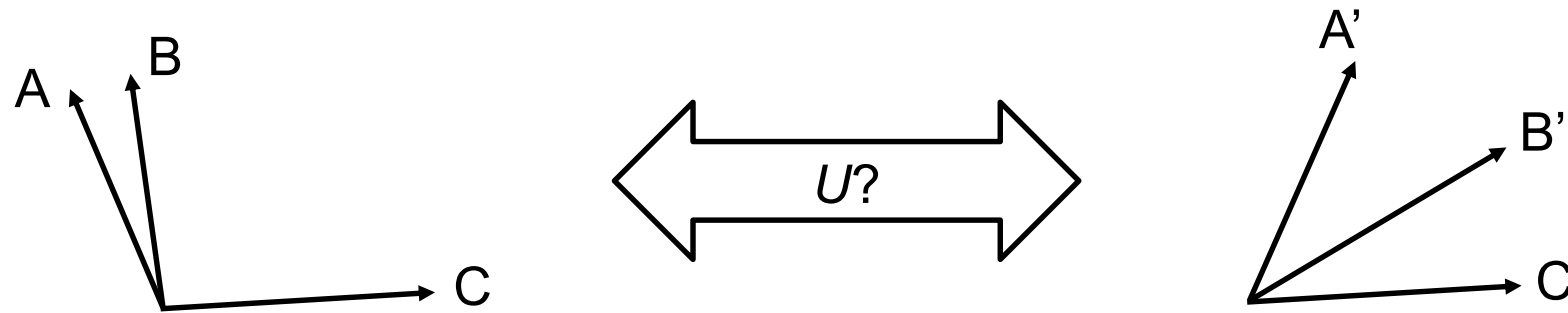
- Oszmaniec-Brod-EG: **cycle test** circuits measure real and imaginary parts of any m -th order Bargmann invariant:



- Circuits previously proposed to measure nonlinear functionals of a single state

[Ekert *et al.*, PRL 88, 217901 (2002)]

- We call a set of unitary-invariants **complete** if it contains enough information to decide any unitary-invariant question about a set of states.
 - Prototypical question:



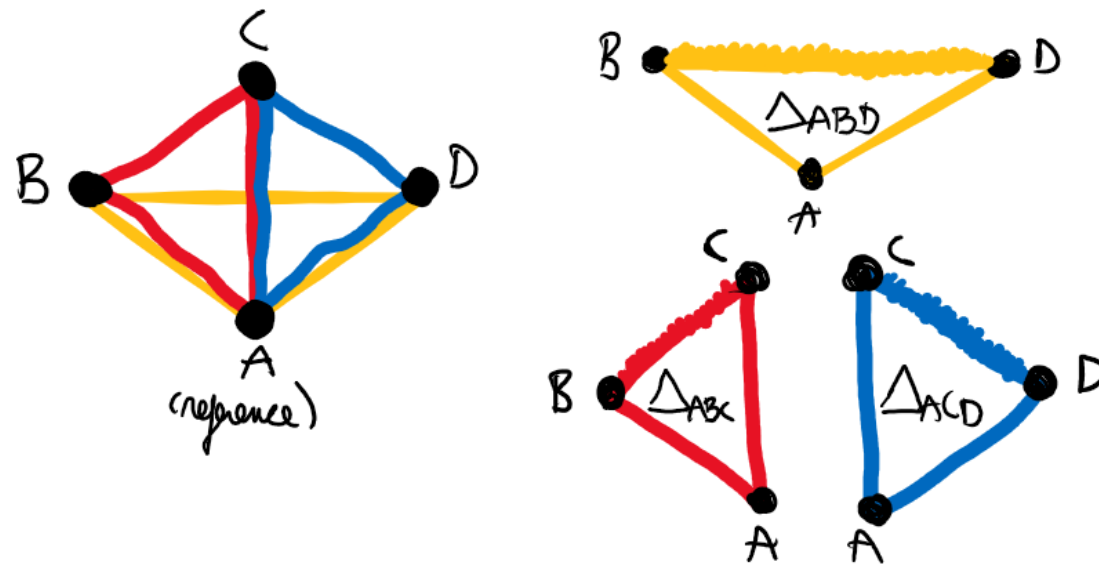
Is there a unitary U that maps one set of states into the other? Such a U exists iff values of invariants in a complete set are the same.

- For N pure states, there are constructions of complete sets using $(N-1)^2$ invariants, of at most N th order.
- For N mixed states you need up to Nd^2+1 invariants, of order up to d^2 .

Gram matrix encodes all unitary-invariant properties of pure states

[Oszmaniec, Brod, EG, arXiv:2109.10006]

- Complete knowledge of unitary-invariant properties enables applications we will describe next.
- In the generic case of non-orthogonal states, characterization is simple:
 - Use all 3-invariants of a reference state with all pairs – “triangulating” the set



$$G = \begin{pmatrix} 1 & \sqrt{\Delta_{12}} & \sqrt{\Delta_{13}} & \sqrt{\Delta_{14}} \\ \sqrt{\Delta_{12}} & 1 & \sqrt{\Delta_{23}}e^{i\phi_{23}} & \sqrt{\Delta_{24}}e^{i\phi_{24}} \\ \sqrt{\Delta_{13}} & \sqrt{\Delta_{23}}e^{-i\phi_{23}} & 1 & \sqrt{\Delta_{34}}e^{i\phi_{34}} \\ \sqrt{\Delta_{14}} & \sqrt{\Delta_{24}}e^{-i\phi_{24}} & \sqrt{\Delta_{34}}e^{-i\phi_{34}} & 1 \end{pmatrix}$$

Where: $\Delta_{ij} = |\langle \psi_i | \psi_j \rangle|^2$

$$\Delta_{1jk} = \langle \psi_1 | \psi_j \rangle \langle \psi_j | \psi_k \rangle \langle \psi_k | \psi_1 \rangle = \sqrt{\Delta_{1j} \Delta_{jk} \Delta_{k1}} e^{i\phi_{jk}}$$

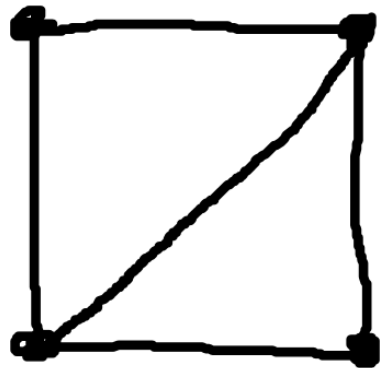
- Information is neatly encoded in the Gram matrix: $G_{ij} \equiv \langle i | j \rangle$

- Phase of $G_{kl} = \text{phase of } \Delta_{rkl}^{\sqrt{\quad}}$ reference state

- All parameters in G are gauge-invariant and can be measured with cycle tests

“Relational information tomography” – example with pair of orthogonal states

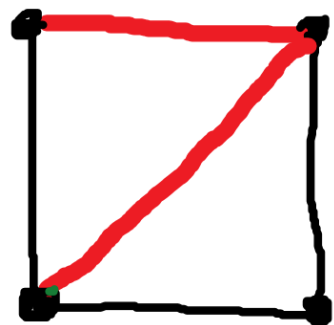
[Ozmaniec, Brod, EG, arXiv:2109.10006]



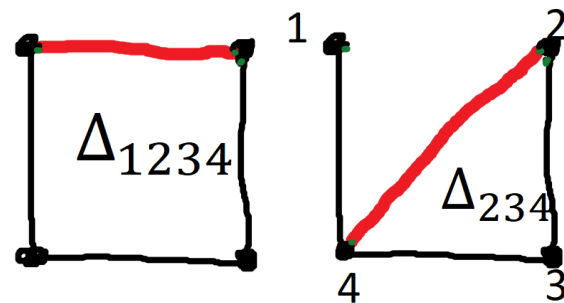
← Vertices = states
edges = measured overlaps: they tell us which higher-order invariants we need to measure

$$\Delta = r e^{i\varphi}$$

- Pick a spanning tree = cycle-free graph containing all vertices



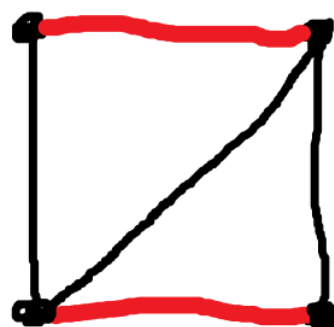
spanning tree
missing edges



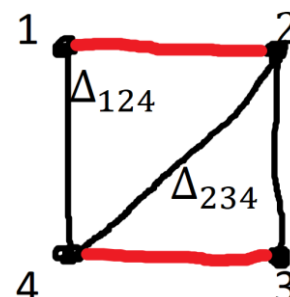
higher-order invariants
to measure

$$G = \begin{matrix} \begin{matrix} 1 & \sqrt{\Delta_{12}} e^{i\varphi_{1234}} & 0 & \sqrt{\Delta_{14}} \\ & 1 & \sqrt{\Delta_{23}} & \sqrt{\Delta_{24}} \\ & & 1 & \sqrt{\Delta_{34}} e^{i\varphi_{234}} \\ & & & 1 \end{matrix} \end{matrix}$$

- Construction is not unique – it’s possible to choose different spanning trees:



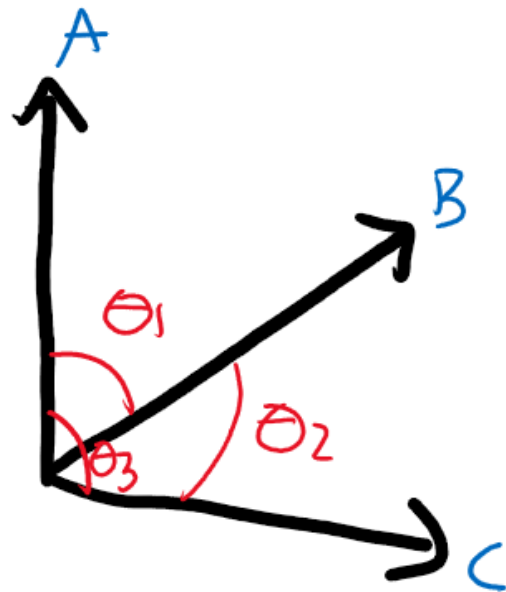
spanning tree
missing edges



higher-order invariants
to measure

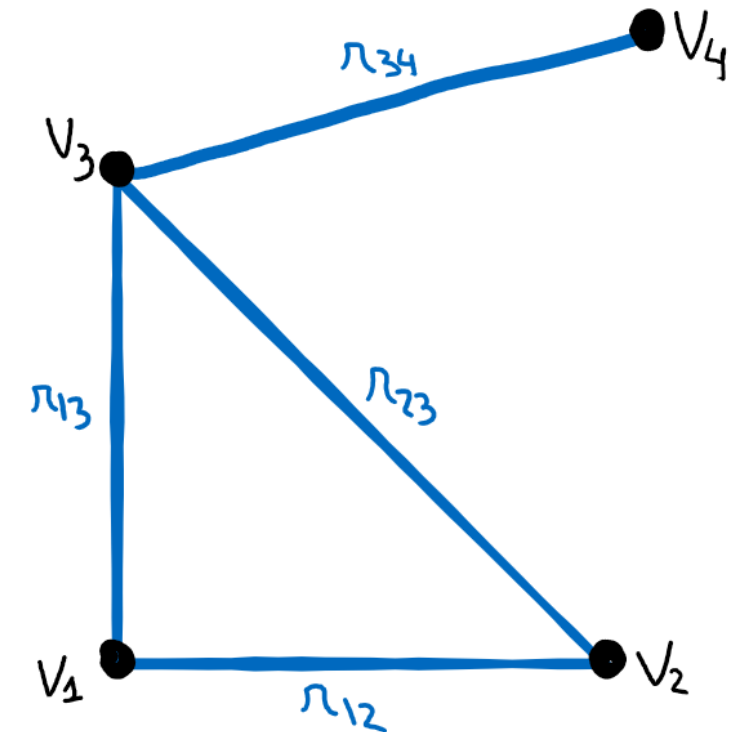
$$G = \begin{matrix} \begin{matrix} 1 & \sqrt{\Delta_{12}} e^{i\varphi_{124}} & 0 & \sqrt{\Delta_{14}} \\ & 1 & \sqrt{\Delta_{23}} & \sqrt{\Delta_{24}} \\ & & 1 & \sqrt{\Delta_{34}} e^{i\varphi_{234}} \\ & & & 1 \end{matrix} \end{matrix}$$

- Basis-independent coherence witnesses
- Noncontextuality inequalities



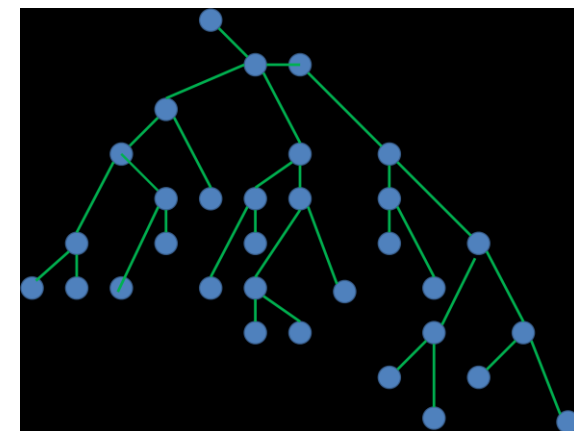
Classicality inequalities for a set of random variables

- **Event graph:** describes probabilistic processes and their correlations:
 - Vertex v_i = probabilistic process yielding outcomes o_{ik} with probability p_{ik}
 - Edge weight r_{ij} = probability that v_i and v_j yield equal outcomes



- Not all edge weights are possible!
 - Boole/Bell/Pitowsky investigated Boole's "conditions of possible experience"
[Pitowsky, Br. J. Philos. Sci. 45 (1), 95 (1994)]

- Cycle-free graphs (trees) impose no constraints on edge weights – for constraints we need cycles



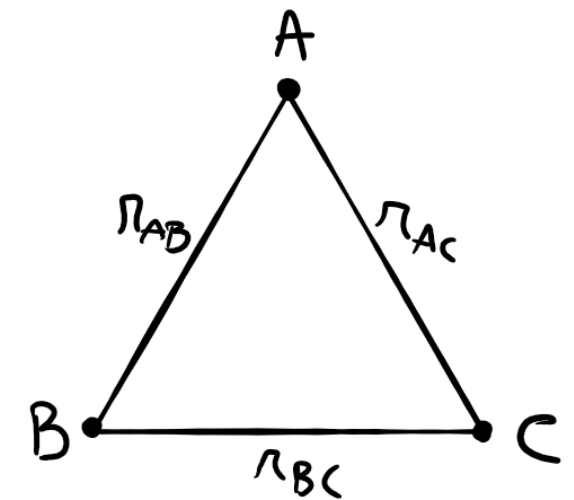
- Let's have a look at the simplest scenario imposing constraints – a 3-cycle graph

3-cycle graph

- Simplest event graph imposing edge weight constraints is the **3-cycle graph**

$$\vec{r} = (r_{AB}, r_{AC}, r_{BC})$$

with $r_{AB} := p(o_A = o_B)$, etc.

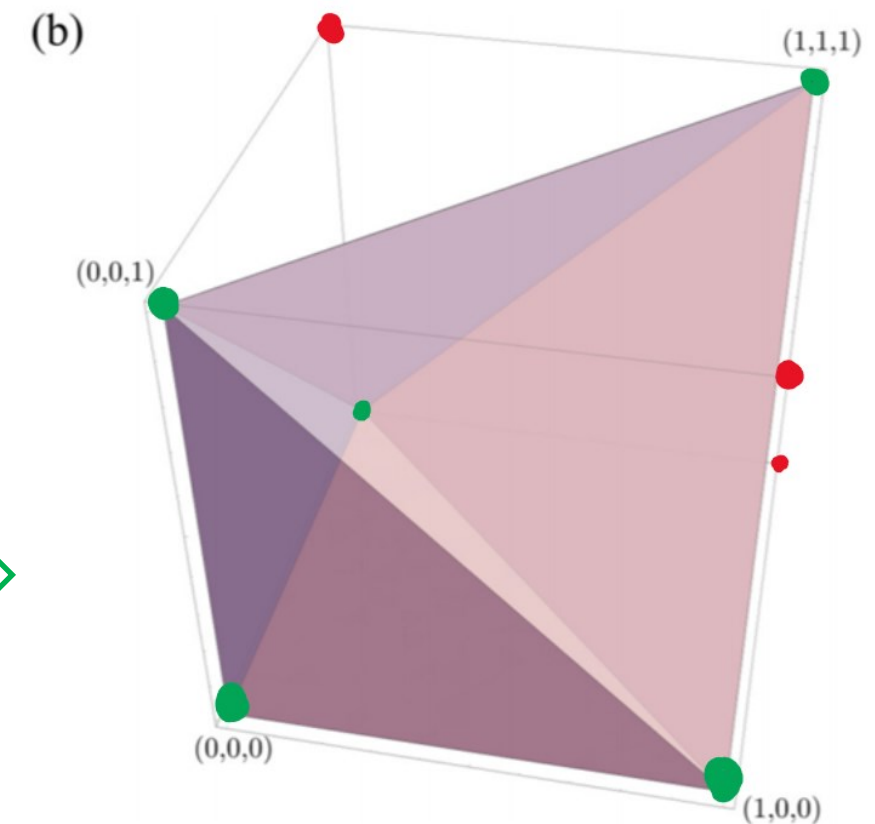


- Some \vec{r} tuples are **impossible**, due to transitivity of equality: $(1, 1, 0)$, $(1, 0, 1)$, $(0, 1, 1)$

- The only **logically allowed states** are those described by convex combinations of the 5 extremal tuples:

$$(0,0,0), (1,1,1), \\ (0,0,1), (0,1,0), (1,0,0)$$

i.e. this polyhedron:



- Now we have 3 non-trivial facets, each describing a linear condition on the correlations (edge weights):

$$r_i + r_j - r_k \leq 1$$

Coherence-free states: diagonal in some reference basis



- Our definition of **classical states** = diagonal, incoherent mixtures of states in some reference basis:

- GLOBAL ρ : DIAGONAL

- LOCAL $\rho_i = \text{Tr}_{\text{ALL } j \neq i}(\rho)$: DIAGONAL

- OVERLAP $r_{ij} = \text{Tr}(\rho_i \rho_j) = \text{PROB. OF EQUAL OUTCOMES OF REFERENCE OBSERVABLE}$

- Example:

$$\rho = \begin{bmatrix} \square & 0 & 0 \\ \square & \rho_{11} & 0 \\ \square & 0 & \rho_{22} \\ \square & 0 & 0 & \rho_{33} \end{bmatrix} \quad \sigma = \begin{bmatrix} \square & 0 & 0 \\ \square & \sigma_{11} & 0 \\ \square & 0 & \sigma_{22} \\ \square & 0 & 0 & \sigma_{33} \end{bmatrix}$$

$$r_{\rho\sigma} = \text{Tr}(\rho\sigma) = \sum_i \rho_{ii} \sigma_{ii} \quad \text{= probability of equal outcomes from measurements of reference observable on the two systems}$$

- For coherence-free states, the overlap has exactly **this interpretation** for edge weights

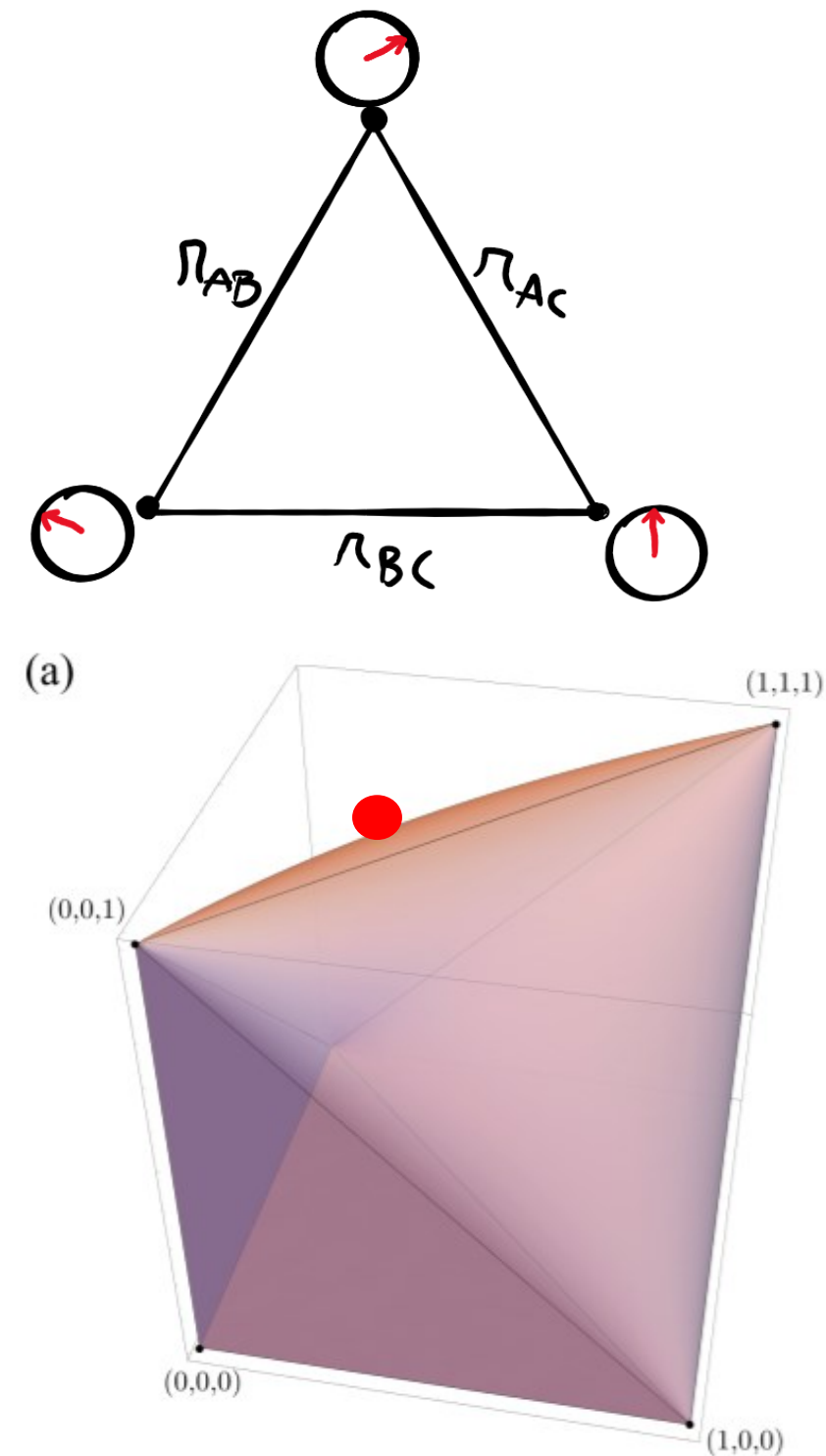
Classical, coherence-free polytope of edge weights

- Vertex: reference basis measurement outcomes on quantum state
- Edge: probability that reference basis measurements give same result for adjacent vertices
- For coherence-free states, we can measure edge weight in two equivalent ways:
 - Direct measurement of reference basis
 - Indirect measurement via SWAP test comparisons
- Now: quantum states may have **coherences** – off-diagonal density matrix entries
- Coherence is witnessed by **violations** of facets of the classical polytope (in indirect, SWAP test measurements)

Theory: [EG, Brod, PRA 101, 062110 (2020)]

Experiment: [Giordani *et al.*, Phys. Rev. Res. 3, 023031 (2021)]

-  = overlap/graph weights violating classical polytope
= **Basis-independent coherence witness**



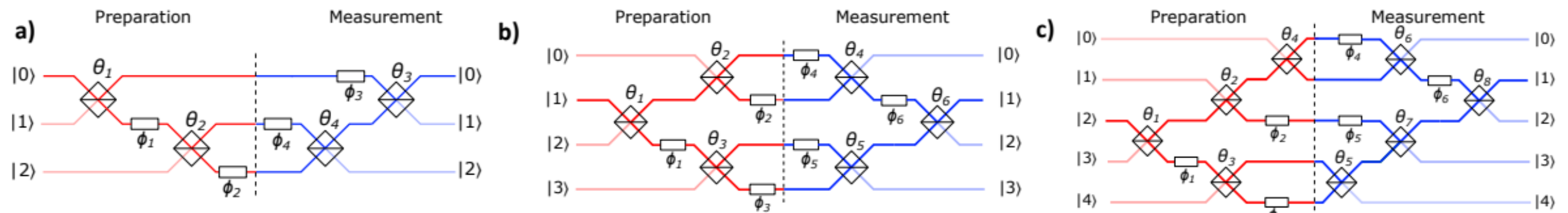
- Rafael Wagner, Rui Soares Barbosa, EG: general framework for obtaining new such coherence witnesses - [arXiv:2209.02670](https://arxiv.org/abs/2209.02670) [quant-ph]

Coherence and dimension witnesses in photonic circuits

Experimental certification of contextuality, coherence and dimension in a programmable universal photonic processor

Taira Giordani,^{1,*} Rafael Wagner,^{2,3,*} Chiara Esposito,¹ Anita Camillini,^{2,3} Francesco Hoch,¹ Gonzalo Carvacho,¹ Ciro Pentangelo,^{4,5} Francesco Ceccarelli,⁵ Simone Piacentini,⁵ Andrea Crespi,^{4,5} Nicolò Spagnolo,¹ Roberto Osellame,⁵ Ernesto F. Galvão,^{2,6,†} and Fabio Sciarrino^{1,‡}

(to appear in Science Advances)



- We used on-chip state preparators/projectors for 1-photon states in m modes, for $m=2,3,4,5$.
- Violation of classicality inequalities from the infinite family described in our arXiv:2209.02670 [quant-ph], witnessing coherence *and* Hilbert space dimension:

$$h_4(r) = r_{0,1} + r_{0,2} + r_{0,3} - r_{1,2} - r_{1,3} - r_{2,3} \leq 1$$

Only violated by states spanning a 3-dimensional space

$$h_n(r) = h_{n-1}(r) + r_{0,n-1} - \sum_{i=1}^{n-2} r_{i,n-1} \leq 1$$

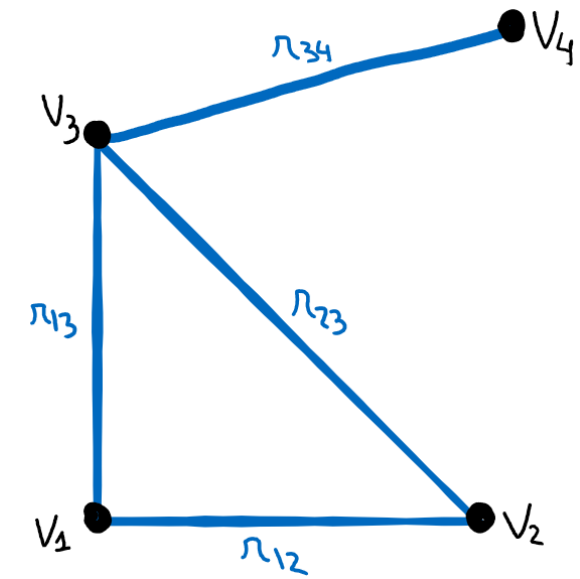
Only violated by states spanning a (n-1)-dimensional space

- Rafael Wagner + Emmanuel Cruzeiro (IST) are investigating finer coherence-witnessing properties of certain classicality inequalities.

Classical polytope facets are noncontextuality inequalities

- General event graph:

- Vertex v_i : probabilistic process yielding outcomes o_{ik} with probability p_{ik}
- Edge weight r_{ij} = probability that v_i and v_j yield equal outcomes



- Classical model is a **global probability distribution function (pdf)** such that:

- All v_i with correct single-process marginal pdfs;
- All pairs of vertices with correct two-vertex marginal pdfs => probability of equal outcomes for neighbouring vertices must match overlap r_{ij}

- Quantum realization of classical model: diagonal density matrices, reference observables reveal pre-existing properties

- Note that the **classical model is non-contextual** – existence of a global pdf is equivalent to non-contextuality

[Abramsky, Branderburger, *N. J. Phys.* **13** (11), 113036 (2011)]

- quantum realization with diagonal states is a way of parameterizing general non-contextual model

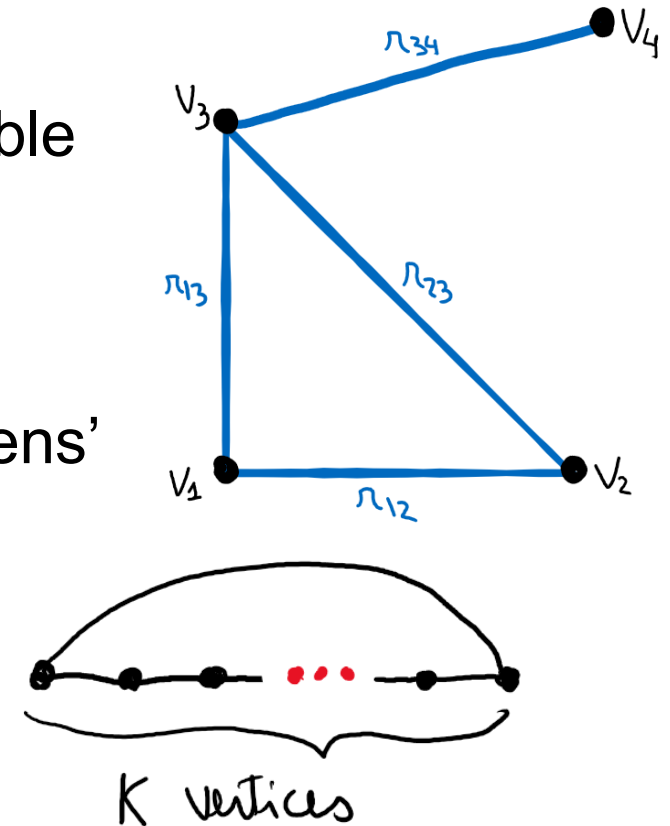
➡ **Classical overlap inequalities are noncontextuality inequalities**

Classical polytope facets are noncontextuality inequalities

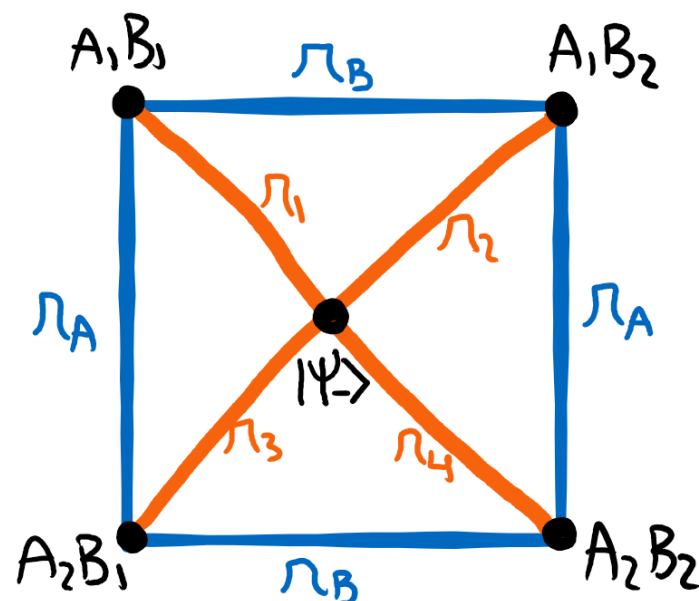
Rafael Wagner, Rui Soares Barbosa, E.G., arXiv:2209.02670 [quant-ph]

- We proved that
 - We recover every non-contextuality inequality obtainable by the exclusivity graph approach
[Cabello, Severini, Winter, PRL112, 040401 (2014)]
 - Violations of cycle inequalities are violations of Spekkens' preparation noncontextuality

$$k\text{-cycle inequalities: } \left(\sum_{i=1}^{k-1} \pi_i \right) - \pi_k \leq k-2$$



- We showed how to computationally obtain facets for arbitrary event graphs.

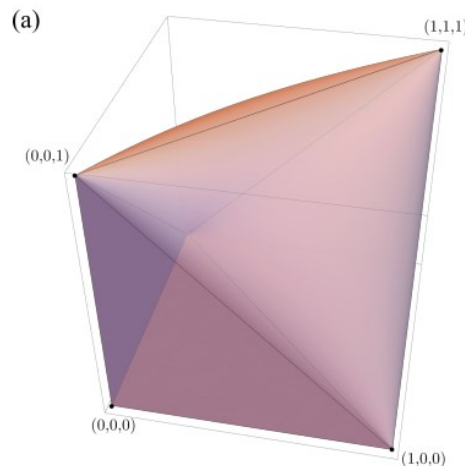


Example: CHSH inequality

- Central vertex: singlet state
- Other vertices: projectors jointly measured by Alice and Bob
- Settings at A and B define r_A, r_B
- 3-cycle inequalities yield the CHSH inequality.

Understanding constraints between different invariants

- For 3 general states, we know the non-trivial bounds that the 3 overlaps must obey:
[E. G., D. J. Brod. Phys. Rev. A 101, 062110 (2020)]

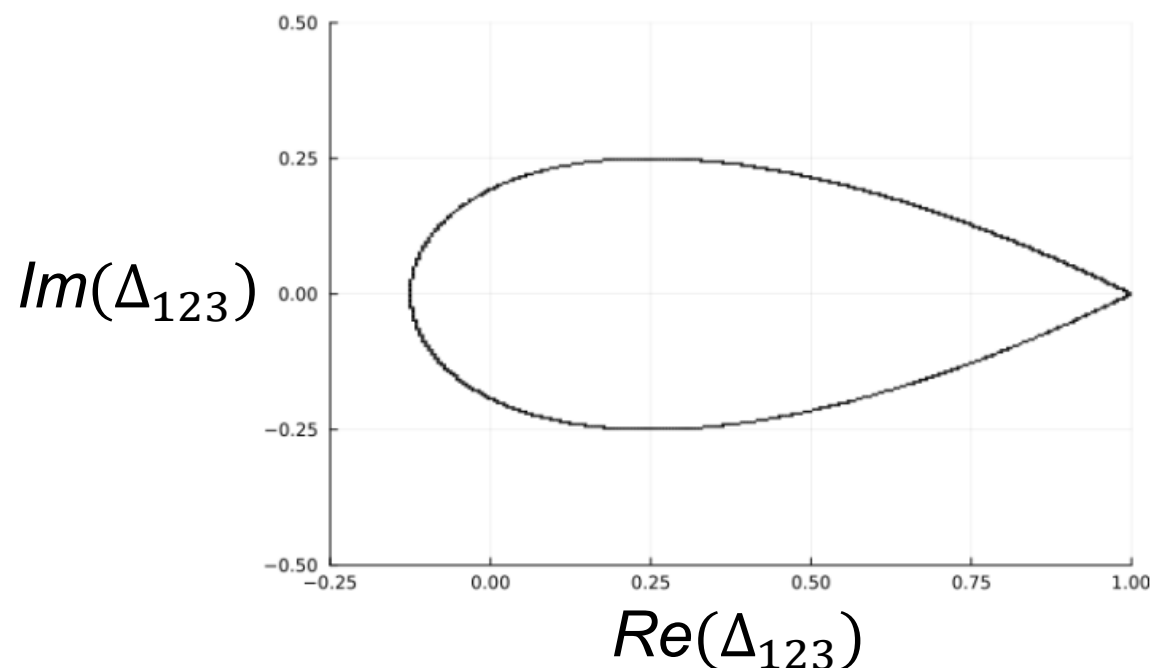


$$r_{AB} + r_{BC} + r_{AC} - 2\sqrt{r_{AB}r_{BC}r_{AC}} \leq 1$$

$$r_{BC} \geq \begin{cases} r_-, & \text{if } r_{AB} + r_{AC} > 1, \\ 0 & \text{otherwise.} \end{cases} \quad r_{\pm} := \left(\sqrt{r_{AB}r_{AC}} \pm \sqrt{(1-r_{AB})(1-r_{AC})} \right)^2$$

- Application in characterization of photonic indistinguishability

- We do not yet have such a complete characterization for overlaps of $N > 3$ states.
- Some partial results: [by Carlos Fernandes]



- We know the boundary:

$$1 - 3r^{\frac{2}{3}} + 2r\cos(\phi) = 0$$

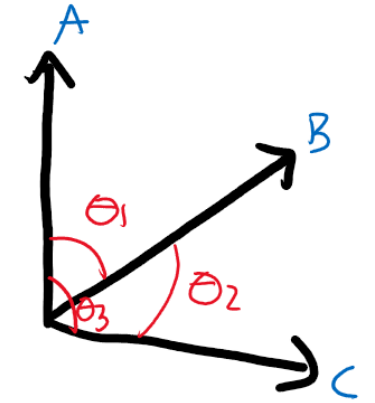
$$\Delta_{123} = re^{i\phi}$$

$$r = \sqrt{\Delta_{12}\Delta_{13}\Delta_{23}}$$

- It grows towards the unit circle as $N \rightarrow \infty$
- Key to obtaining bounds on invariants: $G \geq 0$

- Testing for linear independence
- Witnessing basis-independent imaginarity
- Nonclassicality of Kirkwood-Dirac quasi-probabilities
- Conditions for weak-value anomaly
- Estimating spectra of density matrices
- Out-of-time-ordered correlators (OTOCs)
- Characterization of photonic indistinguishability
- Cycle tests for measuring the scalar spin chirality

- Volume of parallelepiped created by a set of vectors is $V = \sqrt{\det(G)}$
- N states are **linearly independent iff $\det(G) > 0$**



Example with $N=3$:

$$G = \begin{pmatrix} 1 & |\langle \psi_1 | \psi_2 \rangle| & |\langle \psi_1 | \psi_3 \rangle| \\ |\langle \psi_1 | \psi_2 \rangle| & 1 & \langle \psi_2 | \psi_3 \rangle \\ |\langle \psi_1 | \psi_3 \rangle| & \langle \psi_2 | \psi_3 \rangle^* & 1 \end{pmatrix} = \begin{pmatrix} 1 & \sqrt{\Delta_{12}} & \sqrt{\Delta_{13}} \\ \sqrt{\Delta_{12}} & 1 & \sqrt{\Delta_{23}} e^{i\phi_{23}} \\ \sqrt{\Delta_{13}} & \sqrt{\Delta_{23}} e^{-i\phi_{23}} & 1 \end{pmatrix}$$

$$\Delta_{ij} = |\langle \psi_i | \psi_j \rangle|^2$$

$$\Delta_{1jk} = \langle \psi_1 | \psi_j \rangle \langle \psi_j | \psi_k \rangle \langle \psi_k | \psi_1 \rangle = \sqrt{\Delta_{1j} \Delta_{jk} \Delta_{k1}} e^{i\phi_{jk}}$$

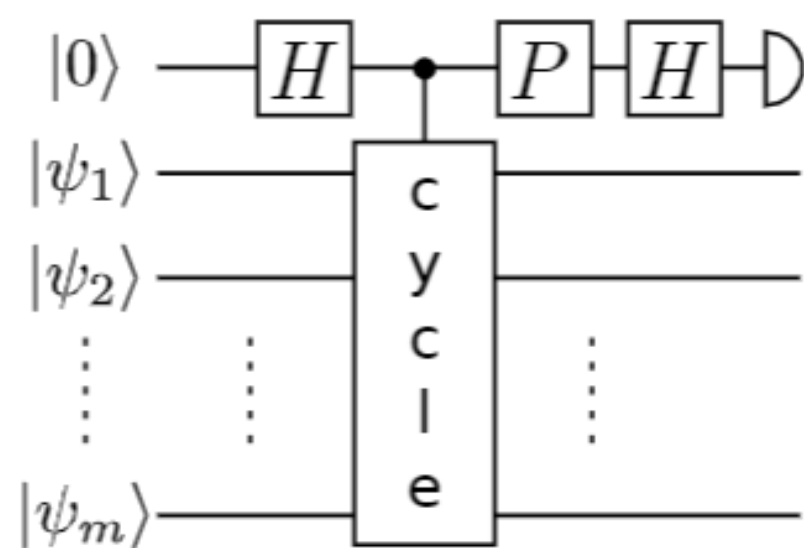
$$\det(G) > 0 \Leftrightarrow 1 - (\Delta_{12} + \Delta_{13} + \Delta_{23}) + 2\sqrt{\Delta_{12}\Delta_{13}\Delta_{23}} \cos(\phi_{23}) > 0.$$

- Possibly useful for dimensionality reduction in machine learning.

- *Imaginaryity*: resource provided by complex numbers in quantum theory
- Recent results show imaginarity is necessary for maximal violation of certain Bell nonlocality scenarios

[M.-O. Renou *et al.*, *Nature* 600, 625 (2021); M.-C. Chen *et al.*, *Phys. Rev. Lett.* 128, 040403 (2022)]

- Cycle test can be used to witness **basis-independent imaginarity**:



$$p(0) = \frac{1 + \text{Im}(\Delta_{12\dots m})}{2}$$

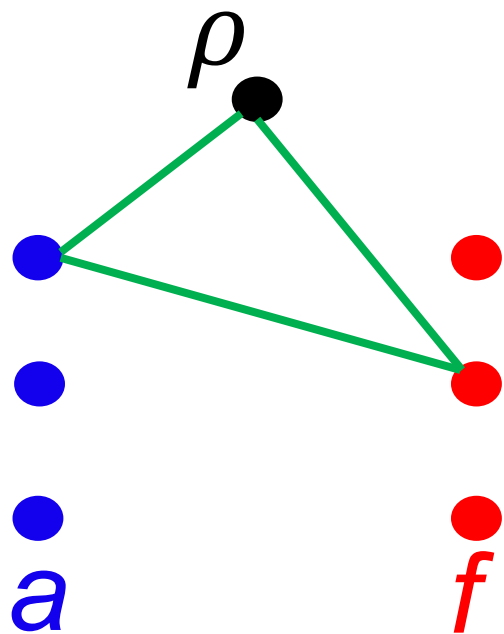
= imaginarity that doesn't "go away" by any choice of basis.

- Rafael Wagner and Felix Ahnefeld (Ulm) are working on a resource theory of basis-independent imaginarity, towards a resource theory of basis-independent coherence (or "set coherence").

- The Kirkwood-Dirac (KD) quasi-probability distribution represents a d -dimensional quantum state - it is normalized but can take negative or complex values.

See e.g. D. R M Arvidsson-Shukur *et al.*, *J. Phys. A: Math. Theor.* **54** 284001 (2021).

- By definition, the value at each phase-space point is a 3rd-order Bargmann invariant of ρ + one basis state from each of two bases a and f :

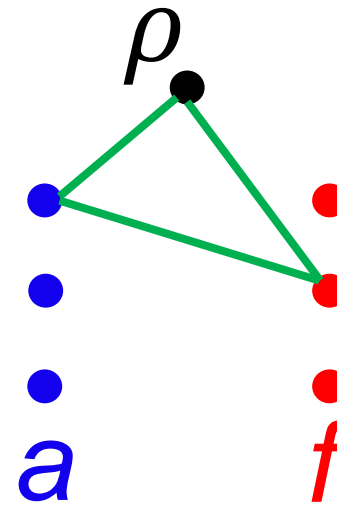


$$\xi(a, f|\rho) := \text{Tr}(\Pi_a \Pi_f \rho)$$

- Cycle test circuits directly measure the KD distribution, with no need for previously proposed weak measurement schemes.

- Results on nonclassicality of KD distribution:

$$\xi(a, f|\rho) := \text{Tr}(\Pi_a \Pi_f \rho)$$



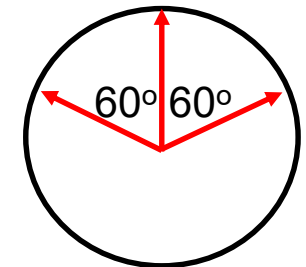
- New observations on non-classicality of value of a single KD phase space point:

- Nonclassicality may arise out of positive third-order invariants, as in the **this example** with $\Delta_{123} = \frac{3}{8}$:

$$|\psi_1\rangle := |0\rangle,$$

$$|\psi_2\rangle := \frac{|0\rangle + \sqrt{3}|1\rangle}{2}$$

$$|\psi_3\rangle := \frac{\sqrt{3}|0\rangle + |1\rangle}{2}$$



- Examples show that only overlaps cannot always decide whether Δ_{123} is a) real or complex; b) positive or negative.
- Using additional assumptions, it's possible to decide negativity/positivity using overlaps only, e.g. when Δ_{123} is both real-valued, and corresponds to one-qubit states.

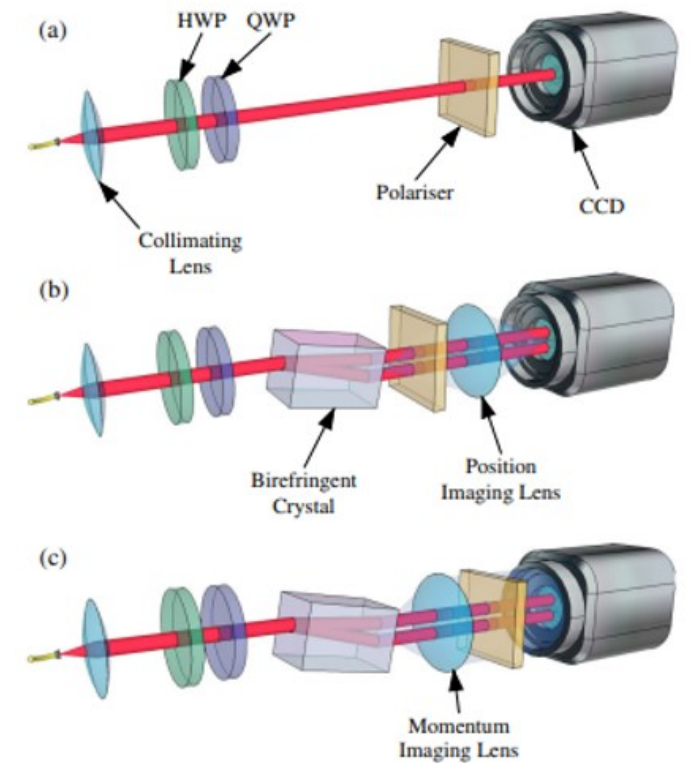
Application: conditions for weak value anomaly

- Weak values of an observable A are measurable quantities associated with:
 - Preparation of a pre-selected state $|\phi\rangle$;
 - “Small” unitary evolution generated by A : $U=\exp(iAt)$;
 - Projective measurement onto post-selected state $|\psi\rangle$;
 - Weak measurement schemes allow estimate of the weak value

$$A_w = \frac{\langle \phi | A | \psi \rangle}{\langle \phi | \psi \rangle}$$

- Anomalous weak values A_w are those outside of the range of A – useful in metrology.

[See J. Dressel *et al.*, *Rev. Mod. Phys.* 86, 307 (2014)]



From Dressel *et al.*, *Rev. Mod. Phys.* 86, 307 (2014)

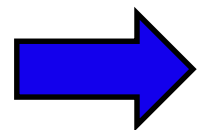
Application: conditions for weak value anomaly

R. Wagner, E.G., PRA 108, L040202 (2023)
R. Wagner *et al.*, arXiv:2302.00705[quant-ph]

- Weak values of an observable A :
$$A_w = \frac{\langle \phi | A | \psi \rangle}{\langle \phi | \psi \rangle}$$
- Weak values are unitary-invariant quantities among pre and post-selected states and eigenvectors of A – measurable using cycle circuits

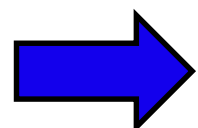
$$A_w = \sum_{a \in \sigma(A)} a \frac{\langle \phi | a \rangle \langle a | \psi \rangle}{\langle \phi | \psi \rangle} = \sum_{a \in \sigma(A)} a \frac{\langle \phi | a \rangle \langle a | \psi \rangle \langle \psi | \phi \rangle}{|\langle \phi | \psi \rangle|^2} = \sum_{a \in \sigma(A)} a \frac{\Delta_3(\phi, a, \psi)}{\Delta_2(\phi, \psi)}$$

- Weak values of A are an average over eigenvalues a_i , weighted by normalized quasi-probabilities g :
$$g(\rho_\phi, \rho_\psi | a_i) := \frac{\Delta_3(\rho_\phi, a_i, \rho_\psi)}{\Delta_2(\rho_\phi, \rho_\psi)}$$



anomalous quasi-probabilities are *necessary* for the appearance of anomalous weak values

- We also showed that anomalous quasi-probabilities require coherence of both ρ_ψ, ρ_ϕ in A 's basis.



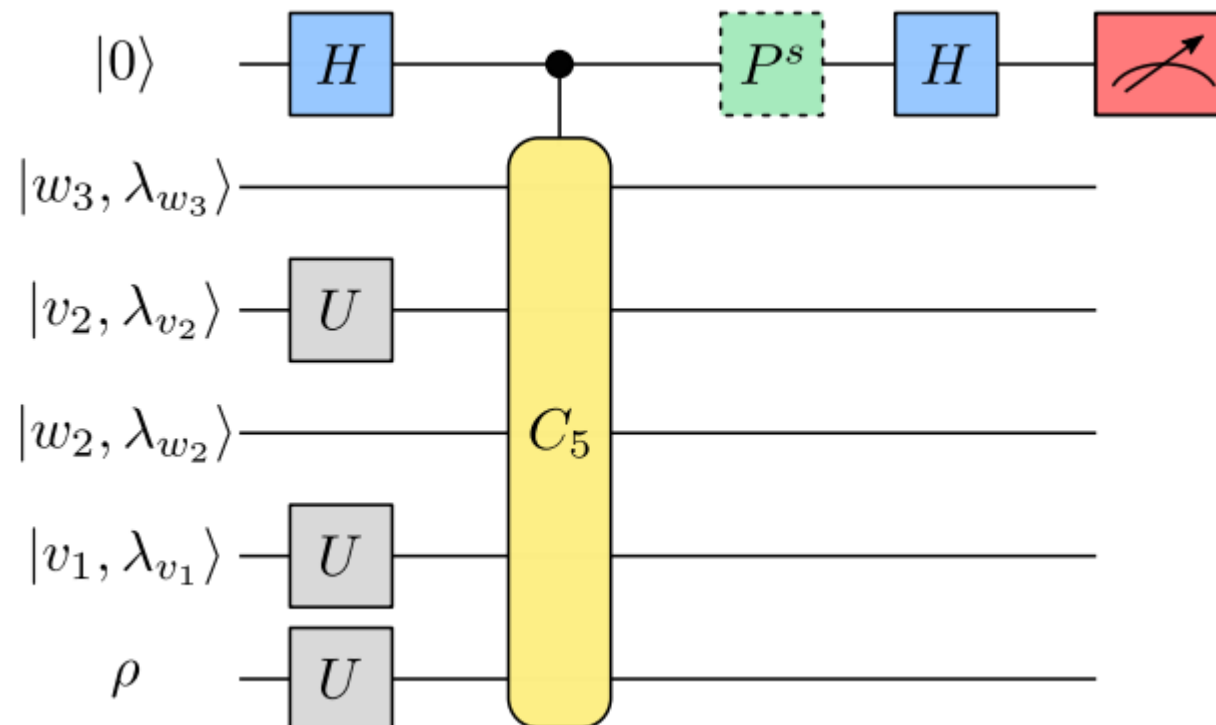
anomalous weak values require coherence of both ρ_ψ, ρ_ϕ in A 's basis

Application: measuring Out-of-Time-Ordered Correlators (OTOCs)

- Out-Of-Time-Ordered Correlators (OTOCs) measure the scrambling of quantum information by tracking how expectation values of initially commuting observables V, W change under unitary dynamics.

$$\text{OTOC}(t) := \text{Tr}(W^\dagger(t)V^\dagger W(t)V\rho)$$

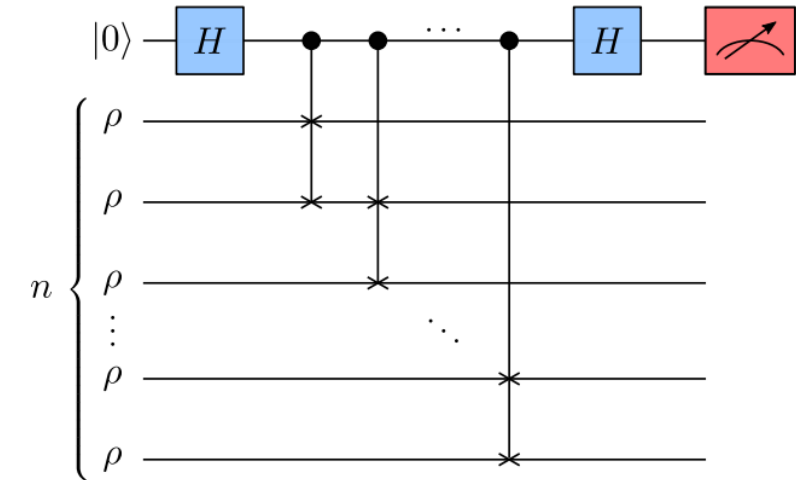
- We noted OTOCs are a function of 5th-order invariants, measurable without the need for inverse U , as proposed previously.



Application: estimating spectra of density matrices

R. Wagner et al., arXiv:2302.00705[quant-ph]

- Cycle test circuit with input of n identical d -dimensional states ρ estimates $Tr(\rho^n)$
- Newton's identities then give us the spectrum of ρ as a function of $Tr(\rho^n)$ for $n = 1 \dots d$



$$\{Tr(\rho^2), Tr(\rho^3), \dots, Tr(\rho^d)\}$$

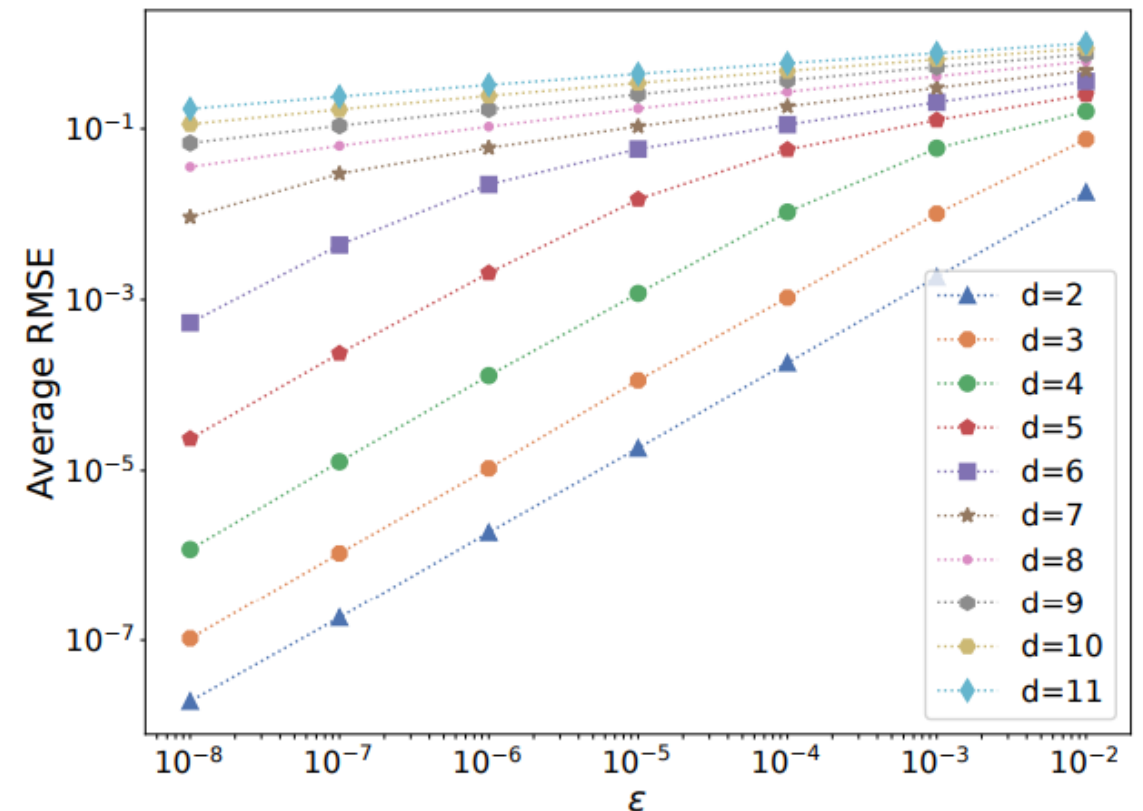
Newton's identities



Spectrum of ρ

- Despite numerical instabilities, method works well for small d . Error in eigenvalue estimation as a function of Gaussian noise ϵ in $Tr(\rho^n)$

Figure 4. Average root-mean-squared error (RMSE) of the estimate for the real part of the eigenvalues of random mixed states, under Gaussian noise ϵ . We start from a data set of exact values of $\Delta_n := Tr(\rho^n)$, $\{\widehat{\Delta}_n\}_{n=2}^d$, introduce Gaussian noise with standard deviation ϵ , and plot the average root-mean-squared error (RMSE) of the estimated eigenvalues under noise. The spectrum reconstruction uses the Faddeev–LeVerrier algorithm based on Newton's identities, and the average RMSE is over 5000 samples, each used to generate 1000 noisy samples. We use the Ginibre random ensemble of mixed states of rank larger than one, employing the algorithm introduced in Ref. [70].



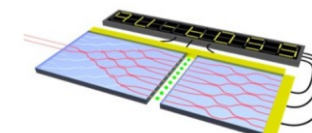
Conclusion

- Unitary invariants give a concise description of all the relational information about a set of projectors
- Helpful for unified discussion of various notions of nonclassicality: basis-independent coherence and imaginarity, contextuality, nonlocality, negativity of quasi-probabilities, anomalous weak values
- Check out our theory papers:
 - E. G., D. J. Brod. Quantum and classical bounds for two-state overlaps. Phys. Rev. A 101, 062110 (2020).
 - M. Oszmaniec, D. J. Brod, E. G. Measuring relational information between quantum states, and applications. ArXiv:2109.10006 [quant-ph].
 - R. Wagner, R. Soares Barbosa, E. G. Inequalities witnessing coherence, nonlocality, and contextuality. ArXiv:2209.02670 [quant-ph].
 - R. Wagner, Z. Schwartzman-Nowik, I. L. Paiva, A. Te'eni, A. Ruiz-Molero, R. Soares Barbosa, E. Cohen, E.G. Quantum circuits measuring weak values and Kirkwood-Dirac quasiprobability distributions, with applications. ArXiv:2302.00705 [quant-ph].
 - R. Wagner, E.G. Simple proof that anomalous weak values require coherence. PRA 108, L040202 (2023).
- And experiments:
 - T. Giordani , C. Esposito, F. Hoch, G. Carvacho, D. J. Brod, E. G., N. Spagnolo , and F. Sciarrino. Witnesses of coherence and dimension from multiphoton indistinguishability tests. Phys. Rev. Res. 3, 023031 (2021).
 - T. Giordani *et al.* Experimental certification of contextuality, coherence and dimension in a programmable universal photonic processor. Science Advances (in press).

• Funding:



Funded by
the European Union



Conclusion



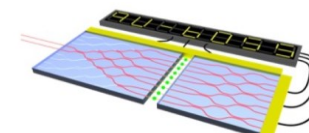
- Unitary invariants give a concise description of all the relational information about a set of projectors
- Helpful for unified discussion of various notions of nonclassicality: basis-independent coherence and imaginarity, contextuality, nonlocality, negativity of quasi-probabilities, anomalous weak values
- Check out our theory papers:
 - E. G., D. J. Brod. Quantum and classical bounds for two-state overlaps. Phys. Rev. A 101, 062110 (2020).
 - M. Oszmaniec, D. J. Brod, E. G. Measuring relational information between quantum states, and applications. ArXiv:2109.10006 [quant-ph].
 - R. Wagner, R. Soares Barbosa, E. G. Inequalities witnessing coherence, nonlocality, and contextuality. ArXiv:2209.02670 [quant-ph].
 - R. Wagner, Z. Schwartzman-Nowik, I. L. Paiva, A. Te'eni, A. Ruiz-Molero, R. Soares Barbosa, E. Cohen, E.G. Quantum circuits measuring weak values and Kirkwood-Dirac quasiprobability distributions, with applications. ArXiv:2302.00705 [quant-ph].
 - R. Wagner, E.G. Simple proof that anomalous weak values require coherence. PRA 108, L040202 (2023).
- And experiments:
 - T. Giordani , C. Esposito, F. Hoch, G. Carvacho, D. J. Brod, E. G., N. Spagnolo , and F. Sciarrino. Witnesses of coherence and dimension from multiphoton indistinguishability tests. Phys. Rev. Res. 3, 023031 (2021).
 - T. Giordani *et al.* Experimental certification of contextuality, coherence and dimension in a programmable universal photonic processor. Science Advances (in press).

Thank you for your attention!

- Funding:



Funded by
the European Union



Fundação para a Ciência e a Tecnologia
MINISTÉRIO DA CIÊNCIA, TECNOLOGIA E ENSINO SUPERIOR

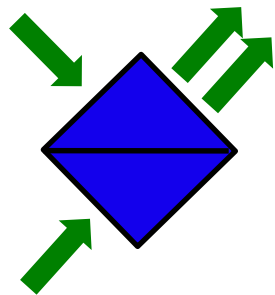
Extra slides

Application: characterizing multi-photon indistinguishability

- Previously: overlaps for multi-photon indistinguishability tests

Brod et al., Witnessing genuine multiphoton indistinguishability. *Phys. Rev. Lett.* 122, 063602 (2019)

Giordani et al., Experimental quantification of genuine four-photon indistinguishability. *N. J. Phys.* 22 043001 (2020)



$$P_b^{AB} = \frac{1 + |\langle A|B \rangle|^2}{2}$$

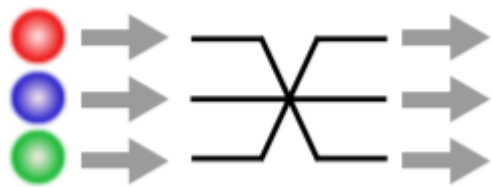
HOM tests measure overlap between spectral wavefunctions, independently of dimension and encoding (polarization, time, colour...)

- Higher-order invariant measurements provide lower bounds for multiple two-photon overlaps:

$$\Delta_{ABC} = \langle A|B \times B|C \times C|A \rangle$$

$$\Rightarrow \Delta_{ij} \geq |\Delta_{ABC}|^2, \quad ij = \begin{cases} AB \\ AC \\ BC \end{cases}$$

- Higher-order invariants can be directly measured using multimode interferometers, e.g. 3-mode balanced tritters (QFT):



$$U = \frac{1}{\sqrt{3}} \begin{pmatrix} 1 & 1 & 1 \\ 1 & e^{i\frac{4\pi}{3}} & e^{i\frac{2\pi}{3}} \\ 1 & e^{i\frac{2\pi}{3}} & e^{i\frac{4\pi}{3}} \end{pmatrix}$$

$$P_{120} = P_{012} = P_{201} = \frac{1}{9} (1 - 2r_{12}r_{23}r_{31} \cos(\varphi + \pi/3))$$

$$P_{021} = P_{210} = P_{102} = \frac{1}{9} (1 - 2r_{12}r_{23}r_{31} \cos(\varphi - \pi/3))$$

[Menssen et al., PRL **118**, 153603 (2017)]

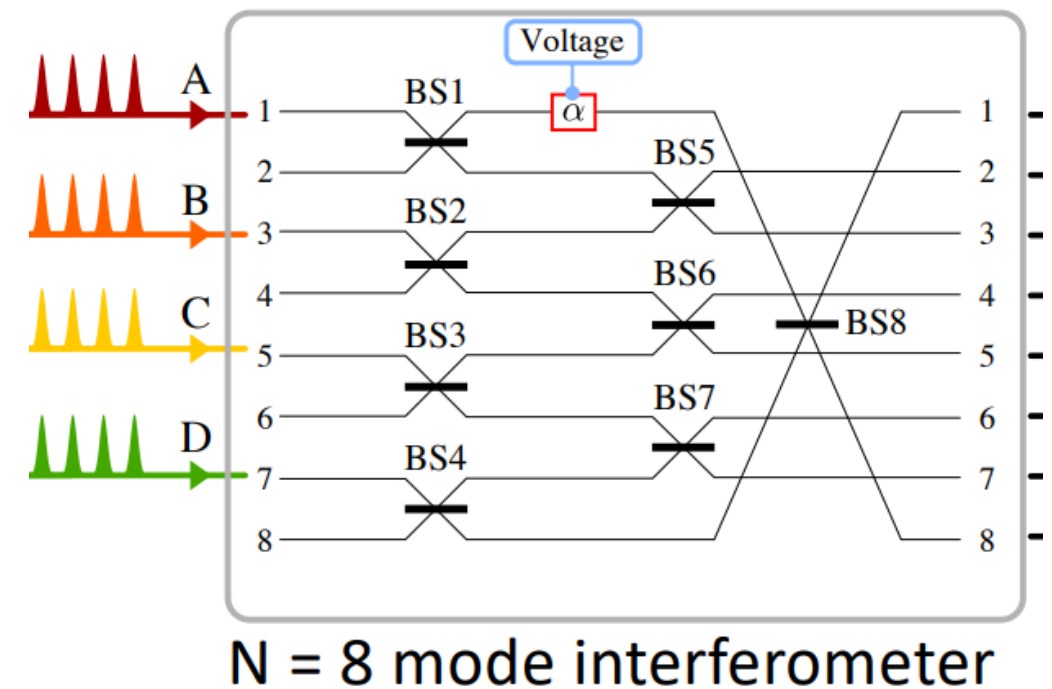
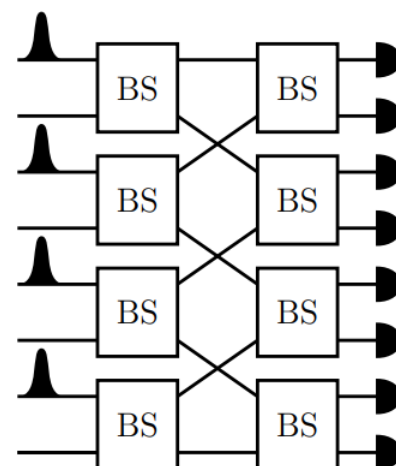
- The output probabilities of any interferometer can be written in terms of invariants only – so generic interferometers will enable estimation of the invariants
Shchesnovich, Bezerra arXiv:1707.03893 [quant-ph]

- Some designs, however, may enable more accurate estimation. An interesting design was recently demonstrated by CNRS/CNR/Rome:

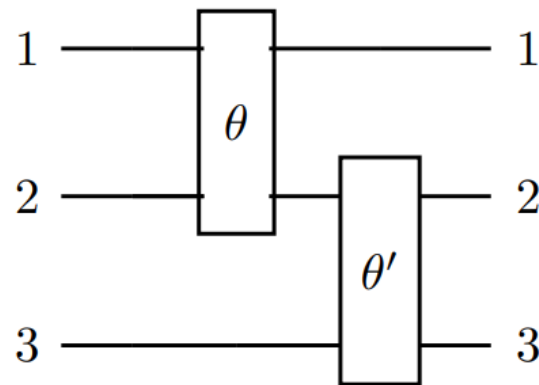
Pont et al, arXiv:2201.13333 [quant-ph]
See also Wu, Sanders, Phys. Rev. Research 4 (2), 023134 (2022)

- Single photons pre- and post-selected on odd modes
- Only two paths to this: either all remain in input, or all move in a cycle – exactly the superposition of possibilities for the cycle test
- Enables measurement of invariants of any order, at high postselection cost

See also Wu, Sanders, Phys. Rev. Research 4, 023134 (2022):



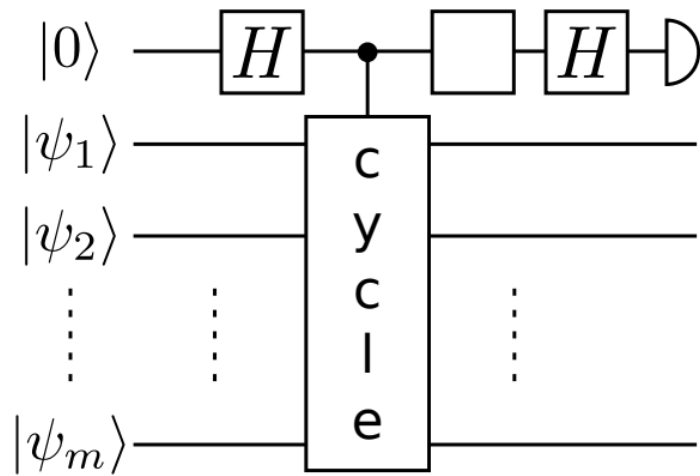
- Some preliminary results – collaboration with Michal Oszmaniec, Carlos Fernandes (INL):
 - For $\text{Re}(\Delta_{ABC})$, two BS are sufficient
 - $|\text{Im}(\Delta)|^2$ can be deduced from that, plus overlaps



- Complete “relational tomography” protocol:
 - Use multiple reconfigurable interferometers to determine all overlaps
 - Pick spanning tree that most decreases the order of the required higher-order invariants
 - Use improved interferometer designs to measure those (e.g. the two BS construction above, for 3rd order invariants)

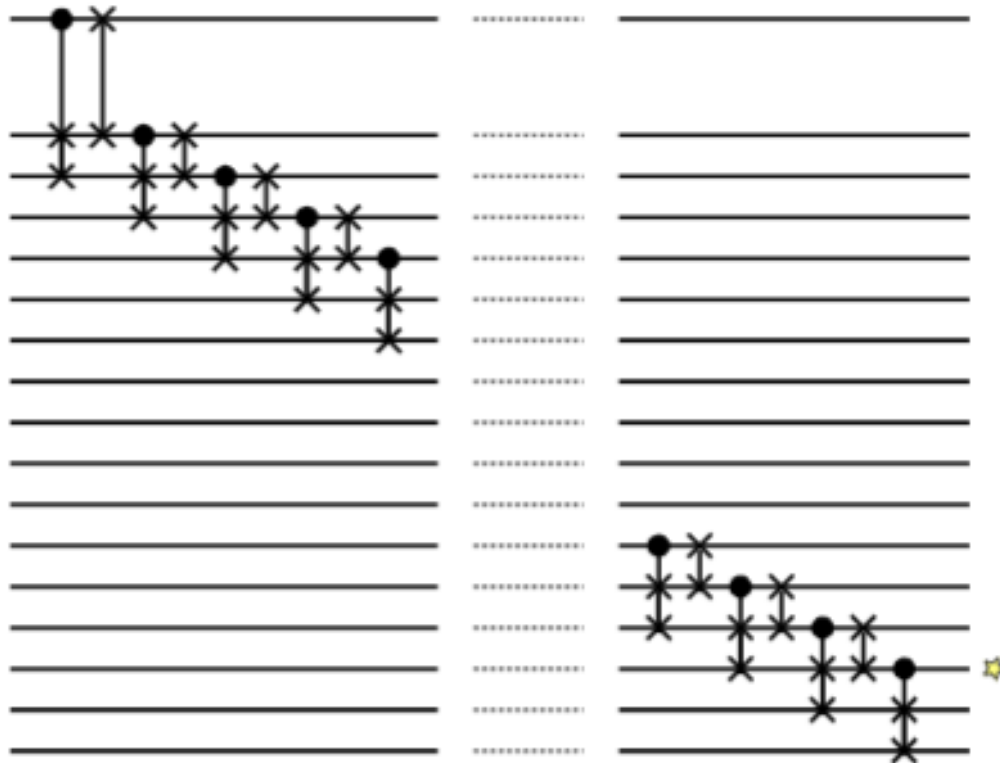
Explicit cycle circuits

Cycle test circuits

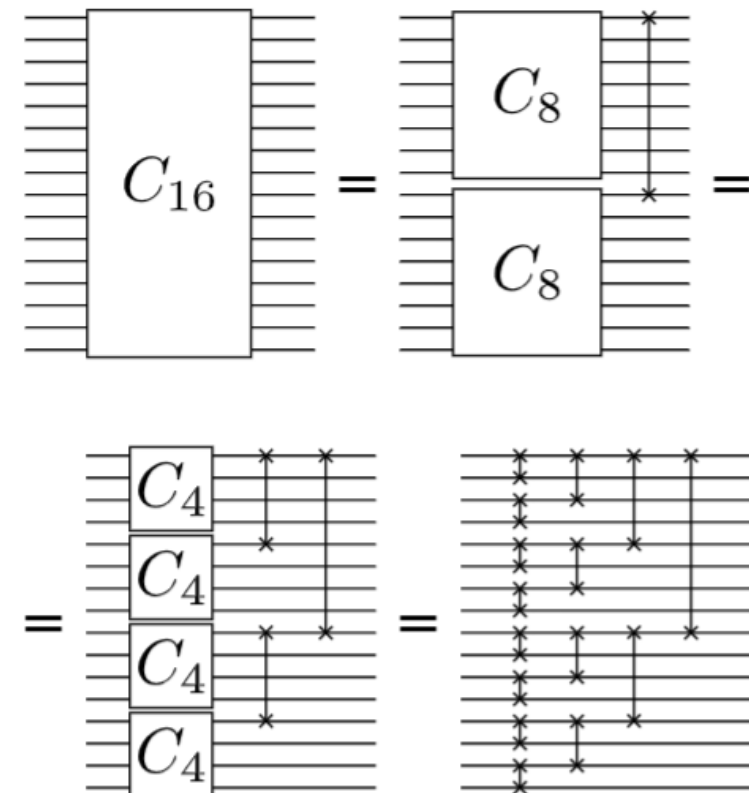


- Controlled-cycle can be decomposed into Fredkin (C-SWAP) gates

- The cycle test circuit can have linear depth (with local C-SWAPs):



- ... or log-depth with long-range C-SWAPs:



- Here's a simple counter-example showing that coherence of ρ_ϕ, ρ_ψ does not guarantee anomalous weak values for A .

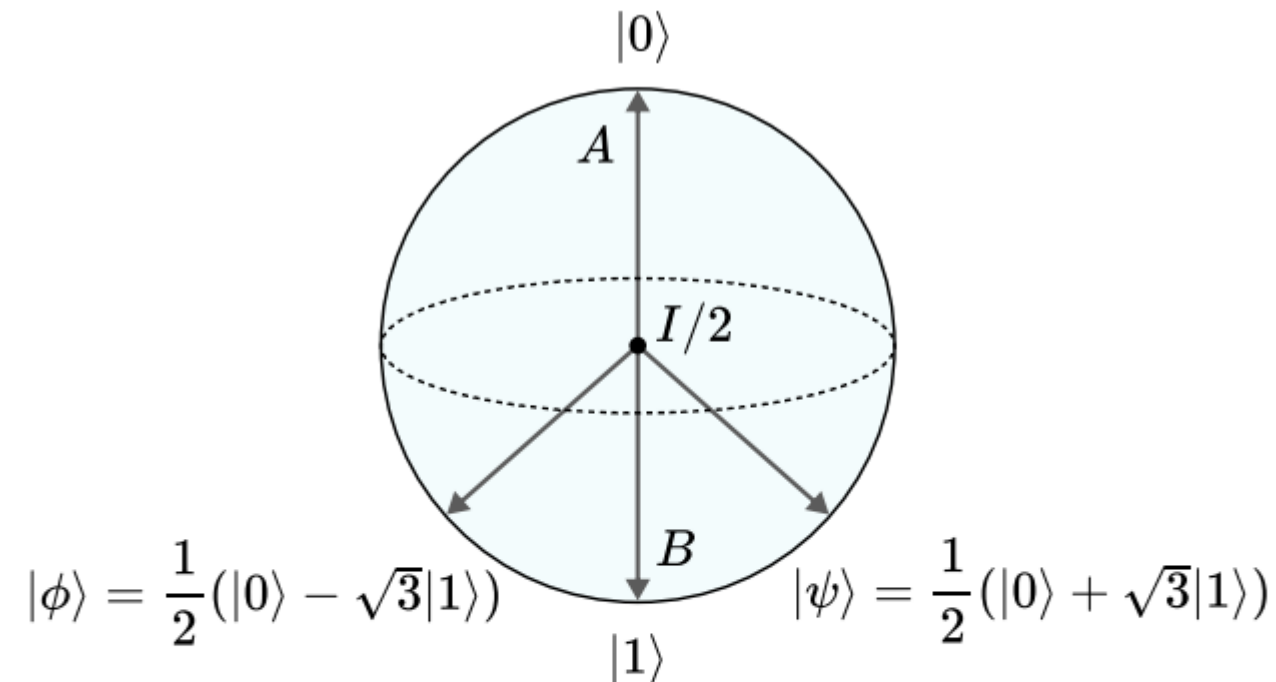
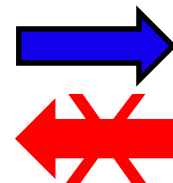


FIG. 2. **Example of anomalous weak values.** The weak value A_w for the projector $A = |0\rangle\langle 0|$, with $|\phi\rangle, |\psi\rangle$ chosen as in the figure, results in the anomalous $A_w = \frac{1}{1/4} \langle \phi|0\rangle\langle 0|\psi\rangle\langle \psi|\phi\rangle = \frac{1}{1/4} \cdot \left(\frac{1}{2}\right) \cdot \left(\frac{1}{2}\right) \cdot \left(-\frac{1}{2}\right) = -\frac{1}{2} < 0$. A similar calculation gives anomalous $B_w = 3/2 > 1$. The weak value of the identity operator is non-anomalous: $I_w = A_w + B_w = 1$.

Anomalous A_w



Coherence of ρ_ϕ, ρ_ψ
in A 's basis